Inorganic Chemistry
Article

Inorg. Chem. **2010**, *49*, 1849–1853 **1849**
DOI: 10.1021/ic902202s

Calibration of Scalar Relativistic Density Functional Theory for the Calculation of Sulfur K-Edge X-ray Absorption Spectra

Serena DeBeer George*,† and Frank Neese*,‡

†*Department of Chemistry and Chemical Biology, Cornell University, Ithaca, New York 14853, and*
‡*Institut für Physikalische und Theoretische Chemie, Universität Bonn, D-53115 Bonn, Germany*

Received November 7, 2009

Sulfur K-edge X-ray absorption spectroscopy has been proven to be a powerful tool for investigating the electronic structures of sulfur-containing coordination complexes. The full information content of the spectra can be developed through a combination of experiment and time-dependent density functional theory (TD-DFT). In this work, the necessary calibration is carried out for a range of contemporary functionals (BP86, PBE, OLYP, OPBE, B3LYP, PBE0, TPSSh) in a scalar relativistic (0^{th} order regular approximation, ZORA) DFT framework. It is shown that with recently developed segmented all-electron scalar relativistic (SARC) basis sets one obtains results that are as good as with large, uncontracted basis sets. The errors in the calibrated transition energies are on the order of 0.1 eV. The error in calibrated intensities is slightly larger, but the calculations are still in excellent agreement with experiment. The behavior of full TD-DFT linear response versus the Tamm−Dancoff approximation has been evaluated with the result that two methods are almost indistinguishable. The inclusion of relativistic effects barely changes the results for first row transition metal complexes, however, the contributions become visible for second-row transition metals and reach a maximum (of an ∼10% change in the calibration parameters) for third row transition metal species. The protocol developed here is ∼10 times more efficient than the previously employed protocol, which was based on large, uncontracted basis sets. The calibration strategy followed here may be readily extended to other edges.

1. Introduction

Noninnocent ligands have continued to receive great attention.[1] Although the existence of ligands in open-shell states has long been realized, it is only recently that the geometric and electronic structures of these systems and the corresponding implications for reactivity have been systematically studied. Among the potentially noninnocent ligands, sulfur-containing systems are the subject of long-standing debates.[1a,b,c−f] Although the terms "oxidation state" and "noninnocence" do not have rigorous quantum mechanical definitions, these concepts are central to chemical reasoning and are consequential for discussing the trends in properties and reactivity among series of related compounds.[2]

It is anything but trivial to a priori recognize a given system as containing noninnocent ligands. Hence one is looking for spectroscopic methods that can be correlated with the concept of noninnocence. For sulfur-containing complexes, one of the most useful approaches is sulfur K-edge X-ray absorption spectroscopy (S−K edge XAS), pioneered in coordination chemistry by Solomon and co-workers.[3] They have demonstrated that the normalized intensity of the Sulfur K-pre-edge peak(s) can be correlated with the involvement of sulfur in the semioccupied and unoccupied valence orbitals.[4] Through careful calibration, one can obtain semiquantitative estimates of metal−ligand covalency.[3−5]

Alternatively, we have recently shown that it is possible to predict sulfur, chlorine, and iron-K-edge spectra on a first-principles basis using time-dependent density functional theory (TD-DFT).[6] In our approach, one solves the time-dependent linear response equations in a subspace of

*To whom correspondence should be addressed. E-mail: sdg63@cornell.edu (S.D.G.); neese@thch.uni-bonn.de (F.N.).

(1) (a) Ray, K.; Petrenko, T.; Wieghardt, K.; Neese, F. *Dalton Trans.* **2007**, 1552. (b) Schrauzer, G. N. *Transition Met. Chem.* **1968**, *4*, 299. (c) McCleverty, J. A. *Prog. Inorg. Chem.* **1968**, *10*, 49. (d) Holm, R. H.; O'Connor, M. J. *Prog. Inorg. Chem.* **1971**, *14*, 241. (e) Eisenberg, R. *Prog. Inorg. Chem.* **1970**, *12*, 295. (f) Gray, H. B. *Transition Met. Chem.* **1965**, *1*, 240. (g) *Dithiolene Chemistry*; Stiefel, E. I., Ed.; Progressin Inorganic Chemistry; Wiley: New York, 2004; Vol. *52*. (h) Pierpont, C. G. Kitagawa, S. In *Inorganic Chromotropism: Basic Concepts and Applications of Colored Materials*; Fukuda; Y., Ed.; Elsevier: Tokyo, 2007; pp 116−142. (i) Hendrickson, D. N.; Pierpont, C. G. In *Topics in Current Chemistry*; Gütlich, P., Goodwin, H. A., Eds.; Springer-Verlag: Berlin, 2004; Vol. *234*, pp 63−95.

(2) (a) Jørgensen, C. K. *Oxidation Numbers and Oxidation States*; Springer: Heidelberg, 1969. (b) Chaudhuri, P; Verani, C. N.; Bill, E; Bothe, E; Weyhermüller, T; Wieghardt, K *J. Am. Chem. Soc.* **2001**, *123*, 2213–2223. (c) Kirchner, B.; Wennmohs, F.; Ye, S.; Neese, F. *Curr. Opin. Chem. Biol.* **2007**, *11*, 131–141.

(3) Shadle, S. E.; Hedman, B.; Hodgson, K. O.; Solomon, E. I. *J. Am. Chem. Soc.* **1995**, *117*, 2259.

(4) (a) Solomon, E. I.; Hedman, B.; Hodgson, K. O.; Dey, A.; Szilagyi, R. K. *Coord. Chem. Rev.* **2005**, *249*, 97. (b) Shadle, S. E.; Penner-Hahn, J. E.; Schugar, H. J.; Hedman, B.; Hodgson, K. O.; Solomon, E. I. *J. Am. Chem. Soc.* **1993**, *115*, 767.

(5) Shadle, S. E.; Hedman, B.; Hodgson, K. O.; Solomon, E. I. *J. Am. Chem. Soc.* **1995**, *117*, 2259.

Published on Web 01/21/2010

particle-hole pairs that only correspond to excitations from the sulfur 1s-core orbitals into the empty valence spin−orbitals. Unlike procedures that are based on the transition state concept,[7] this yields all the relevant excited states as mutually orthogonal in a single calculation. This is computationally much more efficient but does not allow for electronic relaxation (which has been argued to be small at the ligand K-edge[8]). To satisfy the requirements of the sudden approximation,[9] it is necessary to localize the donor orbitals prior to solving the TD-DFT equations. The absolute transition energies obtained in this approach contain significant errors that are characteristic of the particular density functional and the basis set used.[6] This is different from the transition-state-based calculations that tend to predict fairly accurate transition energies[10] (although limited work appears to have been done on transition metal complexes with this methodology). However, the errors of the TD-DFT approach are highly systematic. Thus, following careful calibration it is possible to predict absolute transition energies with an accuracy of a few tenths of an electronvolt. Calculated oscillator strengths (strongly dominated by the electric dipole intensity mechanism[6]) are related to the area under the pre-edge peak for properly normalized experimental spectra. In the interest of generality, it is imperative to pursue an all-electron approach and to include at least kinematic (scalar-) relativistic effects into the calculations. We also note similar calculations in a two-component DFT setting by Ziegler and co-workers.[11]

In our previous work, the BP86 density functional was used together with large, uncontracted basis sets.[6,12,13] Excellent results were obtained for sulfur K-edge spectra together with the scalar relativistic zeroth-order regular approximation (ZORA).[14] The shortcomings of this approach are: (a) the restriction to BP86 and (b) the high computational cost due to the extended basis sets.[6]

This work aims at (a) defining a more efficient computational approach that only requires standard(ized) basis sets, (b) broadening the range of functionals[15] that can be used for the prediction of S−K-edge spectra, (c) comparing the Tamm−Dancoff approximation (TDA)[16] with the full linear response approach, and (d) estimating the importance of scalar relativistic effects.

2. Computational Details

All calculations were performed with a development version of the ORCA quantum chemistry program package.[17] As molecular test set, the six complexes $[M(L^{S,S})_2]^{1-,2-}$ with M = Ni, Pd, Pt ($L^{S,S}$ = benzene-1,2-dithiolate) analyzed earlier were chosen.[12]

2.1. Geometry Optimizations. Unless otherwise noted in the manuscript, the geometries of all complexes were optimized using the BP86 functional, the zeroth-order regular approximation for relativistic effects and the def2-TZVP(-f) basis set in the scalar relativistic recontraction reported in ref 18 (segmented all-electron relativistic basis sets, SARC). For all elements up to bromine, the SARC basis sets are simply scalar relativistic recontractions of the basis sets developed by the Karlsruhe group,[19] while for heavier elements, the primitives and contraction patterns were designed in refs 18. The Coulomb fitting basis set of Weigend[20] was used in uncontracted form in all calculations. The negative charge on the complexes was compensated with the conductor like screening model (COSMO, $\varepsilon = 9.08$) with CH_2Cl_2 taken as the solvent. The calculations used a dense integration grid (ORCA Grid4).

2.2. XAS Calculations. The XAS calculations were done analogously to the geometry optimizations at the optimized BP86/def2-TZVP(-f) geometries. In solving the SCF and TD-DFT equations with hybrid functionals, the RIJCOSX approximation[21] was employed together with standard integration grids. Details of how to perform these calculations are explained in the Supporting Information.

3. Results and Analysis

3.1. Test Systems. As molecular test set, the six complexes $[M(L^{S,S})_2]^{1-,2-}$ with M = Ni, Pd, Pt ($L^{S,S}$ = benzene-1,2-dithiolate) analyzed earlier were chosen.[12] The physical origin of the observed spectra is indicated in Figure 1. In the monoanionic complexes, the bonding is best described as consisting of a square planar low-spin metal d^8 ion bound to a dithiolene radical. Thus, two

(6) (a) DeBeer George, S.; Petrenko, T.; Neese, F. *Inorg. Chim. Acta* **2008**, *361*, 965. (b) DeBeer George, S.; Petrenko, T.; Neese, F. *J. Phys. Chem. A*. **2009**, *112*, 12936.

(7) Triguero, L.; Pettersson, L. G. M.; Agren, H. *Phys. Rev. B* **1998**, *58*, 8097.

(8) Neese, F.; Hedman, B.; Hodgson, K. O.; Solomon, E. I. *Inorg. Chem.* **1999**, *38*, 4854.

(9) (a) Rehr, J. J.; Stern, E. A.; Martin, R. L.; Davidson, E. R. *Phys. Rev. B* **1978**, *17*, 560. (b) Rehr, J. J. *J. Phys.: Condens. Matter* **2003**, *15*, S647.

(10) (a) Slater, J. C. *Adv. Quantum Chem.* **1972**, *6*, 1. (b) Janak, J. F. *Phys. Rev. B* **1978**, *18*, 7165. (c) Stener, M; Lisini, A; Decleva, P. *Chem. Phys. Lett.* **1995**, *191*, 141. (d) Hu, C-H; Chong, D. P. *Chem. Phys. Lett.* **1995**, *262*, 729. (e) Hu, C-H; Chong, D. P. *Chem. Phys. Lett.* **1996**, *262*, 733. (f) Cavalleri, M; Ogasawara, H; Pettersson, L. G. M.; Nilsson, A. *Chem. Phys. Lett.* **2002**, *364*, 363. (g) Han, W. G.; Liu, T. Q.; Lovell, T; Noodleman, L *Inorg. Chem.* **2006**, *45*, 8533. (h) Noodleman, L; Baerends, E. J. *J. Am. Chem. Soc.* **1984**, *106*, 2316. (i) Adams, D. M.; Noodleman, L.; Hendrickson, D. N. *Inorg. Chem.* **1997**, *36*, 3966. (j) Penfield, K. W.; Gewirth, A. A.; Solomon, E. I. *J. Am. Chem. Soc.* **1985**, *107*, 4519.

(11) Casarin, M; Finetti, P; Vittadini, A; Wang, F; Ziegler, T *J. Phys. Chem., A* **2007**, *111*, 5270.

(12) Ray, K.; DeBeer George, S.; Solomon, E. I.; Wieghardt, K.; Neese, F. *Chem.—Eur. J.* **2007**, *13*, 2753.

(13) (a) Sproules, S.; Benedito, F. L.; Bill, E.; Weyhermüller, T.; DeBeer George, S.; Wieghardt, K. *Inorg. Chem.* **2009**, *48*, 10926–10941. (b) Milsmann, C.; Patra, G. K.; Bill, E.; Weyhermüller, T.; DeBeer George, S.; Wieghardt, K. *Inorg. Chem.* **2009**, *48*, 7430. (c) Banerjee, P.; Sproules, S.; Weyhermüller, T.; DeBeer George, S.; Wieghardt, K. *Inorg. Chem.* **2009**, *48*, 5829. (d) Milsmann, C.; Bill, E.; Weyhermüller, T.; DeBeer George, S.; Wieghardt, K. *Inorg. Chem.* **2009**, *48*, 9754.

(14) (a) van Lenthe, E.; Baerends, E. J.; Snijders, J. G. *J. Chem. Phys.* **1993**, *99*, 4597. (b) Van Wüllen, C. *J. Chem. Phys.* **1998**, *109*, 382.

(15) Functionals: B88: Becke, A. D. *J. Chem. Phys.* **1988**, *84*, 4524. OPTX: Hoe, W. M.; Cohen, A. J.; Handy, N. C. *Chem. Phys. Lett.* **2001**, *341*, 319–328. P86: Perdew, J. P. *Phys. Rev. B* **1986**, *33*, 8522. PBE:Perdew, J. P.; Burke, K.; Ernzerhof, M. *Phys. Rev. Lett.* **1996**, *77*, 3865–3868. Hybrid functionals: Becke, A. D. *J. Chem. Phys.* **1993**, *98*, 5648. B3LYP:Devlin, F. J.; Finley, J. W.; Stephens, P. J.; Frisch, M. J. *J. Phys. Chem.* **1995**, *99*, 16883–16902. PBE0: Adamo, C.; Barone, V. *J. Chem. Phys.* **1999**, *110*, 6158–6170. LYP: Lee, C. T.; Yang, W. T.; Parr, R. G. *Phys. Rev. B* **1988**, *37*, 785. TPSS and TPSSh: Tao, J.; Perdew, J. P.; Staroverov, V. N.; Scuseria, G. E. *Phys. Rev. Lett.* **2003**, *91*, 146401. Perdew, J. P.; Tao, J.; Staroverov, V. N.; Scuseria, G. E. *J. Chem. Phys.* **2004**, *120*, 6898. Staroverov, V. N.; Scuseria, G. E.; Tao, J.; Perdew, J. P. *J. Chem. Phys.* **2003**, *119*, 12129.

(16) Hirata, S.; Head-Gordon, M. *Chem. Phys. Lett.* **1999**, *314*, 291.

(17) Neese, F.Becker, U.; Ganyushin, D.; Hansen, A.; Liakos, D. G.; Kollmar, C.; Kossmann, S.; Petrenko, T.; Reimann, C.; Riplinger, C.; Sivalingam, K.; Valeev, E.; Wezisla, B.; Wennmohs, F. *ORCA*, version 2.7.0; University of Bonn: Bonn, Germany, 2009.

(18) (a) Pantazis, D.; Chen, X.-Y.; Landis, C. R.; Neese, F. *J. Chem. Theory Comput.* **2008**, *4*, 908. (b) Pantazis, D.; Neese, F. *J. Chem. Theory Comput.* **2009**, *5*, 2220–2238.

(19) (a) Schäfer, A.; Huber, C.; Ahlrichs, R. *J. Chem. Phys.* **1994**, *100*, 5829. (b) Weigend, F.; Ahlrichs, R. *Phys. Chem. Chem. Phys.* **2005**, *7*, 3297.

(20) Weigend, F. *Phys. Chem. Chem. Phys.* **2006**, *8*, 1057.

(21) (a) Neese, F.; Wennmohs, F.; Hansen, A.; Becker, U. *Chem. Phys.* **2009**, *356*, 98–109. (b) Kossmann, S.; Neese, F. *Chem. Phys. Lett.* **2009**, *481*, 240–243. (c) Neese, F. *J. Comput. Chem.* **2003**, *24*, 1740–1747.

Figure 1. Employed test systems for the S−K-edge XAS calibration $[M(L^{S,S})_2]^-$ (M = Ni, Pd, Pt). Two peaks are observed in the experimental spectra. The higher-energy peak corresponds to a transition from the sulfur 1s core orbital into the d_{xy}-based σ-antibonding molecular orbital. The lower energy peak corresponds to a transition into a predominantly ligand based molecular orbital, reflecting the ligand radical character.

peaks are expected and also observed in the sulfur K-edge spectra. A higher-energy peak reflecting the high lying empty σ-antibonding molecular orbital that shows a significant amount of covalency (depending on the functional and the basis set, the Löwdin population analysis of this orbital shows ~40% (Ni), ~35% (Pd), and ~36% (Pt) metal character).

The transition into the high-lying metal d_{xy}-based σ*-orbital is split into two components in the calculations (see Figure 2). They reflect the "trip-doublet" and "sing-doublet" components[22] that arise from the two ways in which three unpaired electrons can be coupled to a total spin of 1/2.[12] This situation is crudely mimicked in spin-unrestricted TD-DFT calculations via spin-polarization. However, full justice to multiplet effects is not done by spin-unrestricted TD-DFT calculations. Neither the number of multiplet components, their splittings, nor the intensity distribution over the multiplet components is generally correct in spin-unrestricted linear response approaches (see the related discussion in ref 23).

The lower-energy peak reflects the open-shell character of the dithiolene ligand. Its intensity reflects the transition from the sulfur 1s core orbital into a predominantly ligand based π*-orbital that is semioccupied in the monoanionic state. Since this orbital is antibonding between the central metal and the ligands, it reflects a backbonding interaction between a lower-lying formally filled metal d_π orbital with the formally singly occupied ligand orbital. The intensity of this transition is proportional to the sulfur contribution to this molecular orbital and hence reflects the sulfur radical character. In the dianionic complexes this orbital is doubly occupied. Hence, the lower-energy transition disappears and the dithiolene ligands are best regarded as innocent in this oxidation state. This situation and its chemical implications have been discussed at length in ref 12 and will not be repeated here.

3.2. Calibration. The results of the calibration calculations are summarized in Table 1 and the typical agreement that is achieved between theory and experiment is

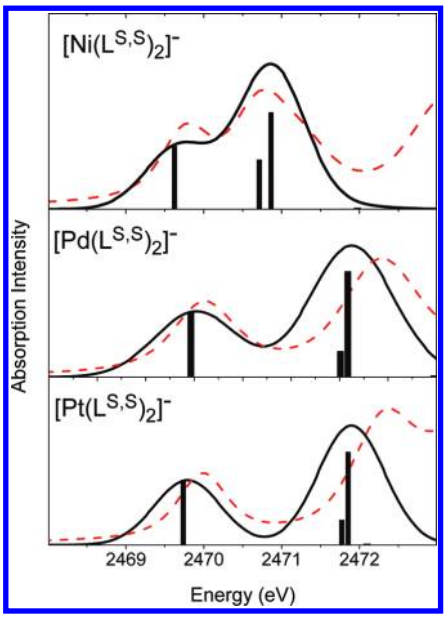

Figure 2. Comparison of calculated scalar-relativistic (black, full lines), and experimental (red, dashed lines) S−K-edge XAS spectra for $[M(L^{S,S})_2]^-$ (M = Ni, Pd, Pt). Experimental intensities were scaled by identical factors for all spectra (fwhm broadening = 1.0 eV, BP86-functional).

Table 1. Calibration Data for TD-DFT-Based Calculations of S−K-Edge Absorption Spectra for Different Density Functionals (ΔE = shift required for the transition energy; b = slope connecting oscillator strength and experimental area, i.e., area = $(1 \times 10^4) f_{osc}/b$)

	ΔE (eV)	B
BP86[a]	60.38 ± 0.12	11.44 ± 0.49
BP86[b]	60.01 ± 0.11	11.49 ± 0.50
BP86[a,c]	76.25 ± 0.15	12.01 ± 0.48
PBE[a]	61.67 ± 0.11	11.18 ± 0.55
PBE[b]	61.33 ± 0.12	11.40 ± 0.50
OPBE[a]	62.75 ± 0.12	11.15 ± 0.53
OPBE[b]	62.41 ± 0.13	11.28 ± 0.54
OLYP[a]	61.83 ± 0.12	11.26 ± 0.52
OLYP[b]	61.49 ± 0.12	11.34 ± 0.51
TPSS[a]	53.53 ± 0.13	11.25 ± 0.50
TPSS[b]	53.18 ± 0.13	11.28 ± 0.50
B3LYP[a]	40.34 ± 0.44	16.83 ± 0.57
PBE0[a]	36.17 ± 0.36	18.03 ± 0.67
TPSSh[a]	44.14 ± 0.18	13.49 ± 0.48

[a] With TDA. [b] Full TD-DFT. [c] Without relativistic corrections.

shown in Figure 2. It should be noted that the experimental intensities are estimated to have an error of ~5% (with contributions from both the normalization and the fitting procedures).[4a] Experimental energies are determined with a precision of ~0.05 eV. It is evident, that the correlation between theory and experiment concerning transition energies and intensities is of excellent quality and as good as previously obtained with the much more elaborate uncontracted basis sets (that are presumed to reflect the basis set limit).[6,12,13] Comparing the value ΔE = 60.38 eV obtained for BP86 functional with ΔE = 61.22 eV obtained previously,[12] it is found that basis set contraction merely leads to a deviation of less than 1 eV or 1−2%. However, the quality of the correlation between theory and experiment is not compromised by the much more compact SARC basis sets. The average error of only ~0.1 eV in the calibrated transition energies is testimony of the excellent behavior of the TD-DFT

(22) (a) Cory, M. G.; Zerner, M. C. *Chem. Rev.* **1991**, *91*, 813. (b) Gouterman, M. *J. Mol. Spectrosc.* **1961**, *6*, 138.
(23) Berry, J. F.; DeBeer George, S.; Neese, F. *Phys. Chem. Chem. Phys.* **2008**, *10*, 4361–4374.

approach for the prediction of S−K-edge XAS. Comparing different functionals with each other, it appears that the predictions of BP86, PBE, OPBE, OLYP and TPSS are of comparable quality. Hybrid- and meta-GGA functionals lead to smaller absolute shifts in the transition energies but also to a larger scatter (consistent with ref 6b). Thus, the considerably increased computational effort (see section 3.5, Timings) that is associated with the hybrid functional does not appear to be well-invested for this application.

The quality of the intensity calibration is similar for all functionals, although it should be noted that hybrid functionals tend to predict larger oscillator strengths for sulfur K-edge transitions. The oscillator strength appears to be proportional to the amount of exact exchange in the functional (TPSSh = 10%, B3LYP = 20%, PBE0 = 25%).

3.3. Full TD-DFT versus Tamm−Dancoff Approximation. Solving the full TD-DFT rather than the simpler TDA equations results in minor changes in the results (the energy shift is reduced by 0.3−0.4 eV). The intensity calibration is essentially unaffected, despite the fact that the full TD-DFT intensities are more rigorous than the TDA ones.[24] In fact, a perturbation theoretical analysis of the analogous random-phase approximation in the Hartree−Fock framework demonstrates that the transition moments in the full TD-DFT approach are correct to first order while those calculated with the Tamm−Dancoff approximation are only correct to zero-th order. Apparently, this slight increase in rigor does not translate into more accurate predictions in core level spectroscopy. Though it is important to note that the experimental intensities have an error of ∼5%, as noted above, and thus better agreement between theory and experiment really cannot be expected.

We note in passing that the transition dipole length- and velocity formalisms lead to virtually indistinguishable results (data not shown). This may turn out to be important for future studies, since the dipole velocity transition moments do not suffer from the gauge problems that were discussed in some detail in ref 6a.

3.4. Scalar Relativistic Effects at the Sulfur K-Edge. As can be seen from Table 1 and Figure 3, the scalar relativistic effects at the sulfur K-edge are limited. Inclusion of scalar relativistic effects improves the energy shift and also slightly improves the correlation with experiment (Table 1). This is an indirect effect that is due to the improved description of the bonding through inclusion of ZORA. Naturally, this is most clearly seen for the heavier systems (see the $[Pt(L^{S,S})_2]^-$ trace in Figure 3). Scalar relativistic effects are known to stabilize s- and p-orbitals and destabilize d- and f-orbitals on heavier metals.[25] These changes in the energies of the important metal orbitals must, of course, have an influence on the covalency of the metal−ligand bonds and therefore also on the XAS intensities. However, even for the heaviest metal in this study (Pt in $[Pt(L^{S,S})_2]^{-,2-}$) the effects are limited. To some extent this is due to the calibration procedure that,

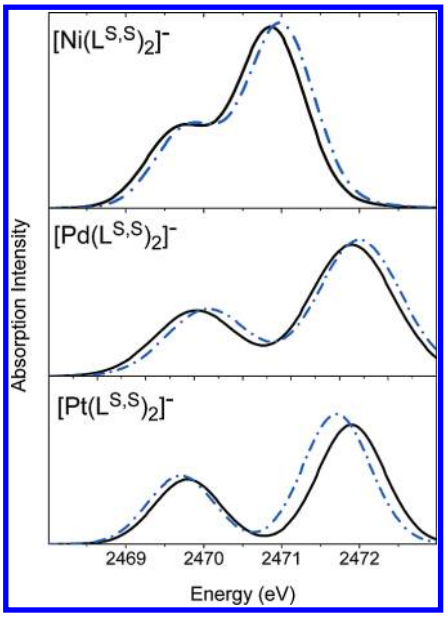

Figure 3. Comparison of calculated scalar-relativistic (black, full lines), and calculated nonrelativistic (blue, dash-dot lines) S−K-edge XAS spectra for $[M(L^{S,S})_2]^-$ (M = Ni, Pd, Pt) (fwhm broadening = 1.0 eV, BP86-functional).

in an average way, compensates for the lack of relativistic effects in the corresponding traces of Figure 3. In an absolute sense, the effects are larger. The scalar relativistic corrections bring the calculated transition energies on average ∼16 eV closer to experiment. Likewise, the calibration constant for the oscillator strengths is ∼10% larger for the nonrelativistic calculations. This can be explained by looking at the calculated orbital compositions. In fact, the calculated Pt character in the σ-antibonding d_{xy}-based orbital increases by 1.8% (from 34.5% to 36.3%) upon going from the nonrelativistic to the ZORA calculations, whereas for the semioccupied ligand-based orbital, the Pt character increases from 17.6% (NonRel) to 20.8% in the ZORA calculations. Because of the smaller metal character in the acceptor orbitals, the sulfur character increases correspondingly in the nonrelativistic calculations and hence the intensities increase by ∼10% in keeping with the changes in the orbital compositions. Taken together, the scalar relativistic effects at the sulfur K-edge are limited and indirect. Not even toward the end of the third transition row do the effects exceed 10%. Thus, even nonrelativistic calculations that replace the deep metal core electrons by effective core potentials (ECPs) might well be successful for calculations at the S K-edge. However, the computational cost of the scalar relativistic ZORA calculations with the SARC basis sets is not much higher than corresponding calculations with accurate small core ECPs. Hence, we prefer to utilize the higher consistency and generality of the scalar relativistic approach which can be applied in the same way to both ligand- and metal K-edges.

3.5. Timings. To demonstrate the timing advantages of the "new" standard protocol for the calculation of S−K-edge spectra (and by inference also for the calculation of other edges), we have calculated a slightly larger complex: $[W(L^{S,S})_3]$ (see Figure 4), formally at the W(VI) level. The geometry of the complex was optimized with the BP86

(24) For reviews see(a) Neese, F. *Coord. Chem. Rev.* **2009**, *253*, 526. (b) Dreuw, A; Head-Gordon, M. *Chem. Rev.* **2005**, *105*, 4009.

(25) Strange, P. *Relativistic Quantum Mechanics*; Cambridge University Press: Cambridge, U.K., 1998.

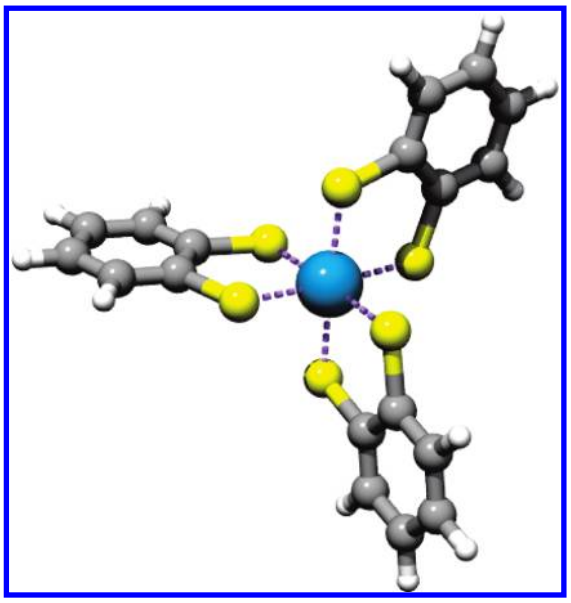

Figure 4. Complex $[W(L^{S,S})_3]$ used for the timing comparisons between the "old" and "new" standard protocols for the calculation of S−K-edge spectra. Molecular symmetry was not used in the calculations.

functional, the SV(P) basis set[19] and a Stuttgart-Dresden effective core potential for W.[26] We note in passing that using a simple molecular mechanics starting structure, this calculation took 8 min for 8 geometry cycles on four cores of a MacPro 3.1 equipped with 2 quad-core Intel XEON 3.0 GHZ CPUs.

Using the new standard protocol (including the COSMO model with a CH_2Cl_2 solvent) together with the def2-TZVP(-f) basis set, the system is described by 813 basis functions and 2052 auxiliary functions. On five cores of the same computer as described above, the SCF calculation with the BP86 functional takes 5.5 min (25 SCF cycles) and the calculation of 5 TD-DFT roots requires 2.8 min.

By contrast, the old standard protocol requires tightened integration accuracy and large uncontracted basis sets. In this case, there are 1591 basis functions and 2179 auxiliary basis functions. The convergence of the SCF equations is noticeably poorer because of the large uncontracted basis sets and requires 139 min (107 cycles). The calculation of five TD-DFT roots requires 19.6 min.

Thus, overall, the new protocol is more than a factor of 10 more efficient than the old protocol, while the accuracy of the predictions is not inferior. Hence, it is computationally much more attractive and consistent than the previously used approach. For hybrid functionals like B3LYP, the computational savings are even more dramatic due to implementation of the RIJCOSX approximation that is fully characterized in ref 21. Using the new standard protocol together with the B3LYP functional, the calculations take just 42 min, whereas the analogous calculation with the old approach is barely feasible.

4. Concluding Remarks

In conclusion, the present work defines a TD-DFT protocol for the accurate calculation of S−K-edge spectra in an efficient, standardized way that applies to molecules comprised from atoms from all over the periodic table and using a broad variety of modern density functionals. This is important because it is frequently required that spectroscopic observables are calculated at the same level of theory as other properties (such as total energies). The methodology is implemented in a user-friendly way into the freely available ORCA[17] program. Future work will concentrate on extending this methodology to the calculation of the K-edges of other elements and, in particular, to the calculation of other edges and novel X-ray experiments.

Acknowledgment. S.D.G. thanks the Department of Chemistry and Chemical Biology at Cornell University for generous financial support. F.N. gratefully acknowledges financial support from the University of Bonn, the SFB 624, the SFB 813 and the priority program SPP 1319.

Supporting Information Available: A generic ORCA input file, nonrelativistically recontracted SARC bases, and optimized geometries (PDF). This material is available free of charge via the Internet at http://pubs.acs.org.

(26) Andrae, D.; Haeussermann, U.; Dolg, M.; Stoll, H.; Preuss, H. *Theor. Chim. Acta* **1990**, *77*, 123.